Quantum noise of a white-light cavity using a double-pumped gain medium

Yiqiu Ma, Haixing Miao, Chunnong Zhao, and Yanbei Chen

Phys. Rev. A **92**, 023807 — Published 5 August 2015

DOI: 10.1103/PhysRevA.92.023807

Quantum noise of white light cavity using double-pumped gain medium

Yiqiu Ma,[1] Haixing Miao,[2] Chunnong Zhao,[1] and Yanbei Chen[3]

[1]*School of Physics, University of Western Australia, WA 6009, Australia*
[2]*School of Physics and Astronomy, University of Birmingham, B15, 2TT, United Kingdom*
[3]*Theoretical Astrophysics 350-17, California Institute of Technology, Pasadena, CA 91125, USA*

Laser interferometric gravitational-wave detectors implement Fabry-Perot cavities to increase their peak sensitivity. However, this is at the cost of reducing their detection bandwidth, which originates from the propagation phase delay of the light. The "white-light-cavity" idea, first proposed by Wicht *et al.* [Optics Communications **34**, 431 (1997)], is to circumvent this limitation by introducing anomalous dispersion, using a double-pumped gain medium, to compensate for such a phase delay. In this article, starting from the Hamiltonian of the atom-light interaction, we apply an input-output formalism to evaluate the quantum noise of the system. We find that apart from the additional noise associated with the parametric amplification process noted by others, the stability condition for the entire system poses an additional constraint. By surveying the parameter regimes where the gain medium remains stable (not lasing) and stationary, we find that there is no net enhancement of the shot–noise–limited sensitivity. Therefore, other gain media or different parameter regimes should be explored for realizing the white light cavity.

PACS numbers:

I. INTRODUCTION

Second generation large-scale interferometric gravitational wave detectors, such as advanced LIGO [1], advanced VIRGO [2], and KAGRA [3], are designed to operate at better sensitivity than the first generation detectors. This improvement in sensitivity comes from an increase in the optical power and the introduction of a signal recycling mirror (SRM) to the initial configuration [4]. The SRM at the dark port forms a signal recycling cavity with the input test mass mirror (ITM). The position of the SRM determines the propagation phase of the signal light inside the signal recycling cavity, and control of the SRM parameters allows for adjustments to the frequency response of the interferometer [5, 6]. Two typical operational modes are the *signal recycling mode* and the *resonant sideband extraction mode*. The signal recycling mode enhances the sideband field which carries the gravitational wave signal inside the cavity, while the resonant sideband extraction mode increases the detection bandwidth which is the effective bandwidth of the combined signal recycling cavity and arm cavity [7].

However, broadening the detection bandwidth in the resonant sideband extraction mode comes at a loss of the peak sensitivity; while enhancing the peak value of the sensitivity in the signal recycling cavity results in a narrower detection bandwidth. This trade-off is represented by the integrated sensitivity [7]:

$$\int_0^{\omega_{\rm FSR}} \frac{1}{S_{hh}(\Omega)} d\Omega = \frac{2\pi L_{\rm arm} P_c \omega_p}{\hbar c}, \tag{1}$$

which only depends on the intra-cavity power P_c and the cavity length $L_{\rm arm}$, and is independent of the properties of the signal recycling cavity. The $S_{hh}(\Omega)$ is the quantum shot–noise–limited sensitivity spectrum [8] and the ω_p, c and Ω here are the laser frequency, the speed of light and the sideband frequency of the light field, respectively. The angular frequency $\omega_{\rm FSR} = \pi c/L_{\rm arm}$, which is the free spectral range of the arm cavity of the interferometer. Here, we only consider the shot–noise–limited strain sensitivity since radiation pressure noise can in principle be evaded using frequency-dependent readout or sufficiently heavy test masses. Such a trade-off between bandwidth and peak sensitivity is due to the relative phase shift between the sideband field and the carrier light propagating inside the arm cavity. There are several proposals in the literature that try to achieve the resonant amplification of the signal without decreasing the bandwidth, by using the idea of the *white light cavity*. Among these, Wicht *et al.* were the first to suggest placing an atomic gain medium with anomalous dispersion inside the signal recycling cavity to cancel the propagation phase [9, 10]. This idea was then followed by Pati and Yum *et al.* with different types of active media [11–13].

The anomalous dispersion phenomenon and the interesting "superluminal" physics of the propagation of a light pulse in these active media have been theoretically discussed [14] and experimentally demonstrated [15, 16]. In these experiments, the anomalous dispersion is usually realized by using a double-pumped gain medium in which the anomalous dispersion lies in between the two gain peaks. The gain medium with anomalous dispersion is subject to an additional quantum noise that accompanies the amplification process. The effect of this additional quantum noise on the observability of "superluminal" pulse propagation effect has been discussed in [17–20]. In particular, Refs. [17, 20] gave a general discussion of this noise using Caves' theory of the amplifier [21], which based on the general requirement that the field operator should satisfy bosonic commutation relation, without providing a complete analysis of the dynamical origin of this noise. Ref. [19] discussed a more concrete example of the field propagation inside a medium consisting of pumped two-level atoms. However, the effect of this additional noise on the sensitivity of of the gravitational wave detector designs proposed in [9–13] was not analyzed before. Moreover, to study the detector designs containing the double gain medium, Caves' method can not be directly applied the since the additional noise has two frequency channels, as we shall show in Section III of this paper.

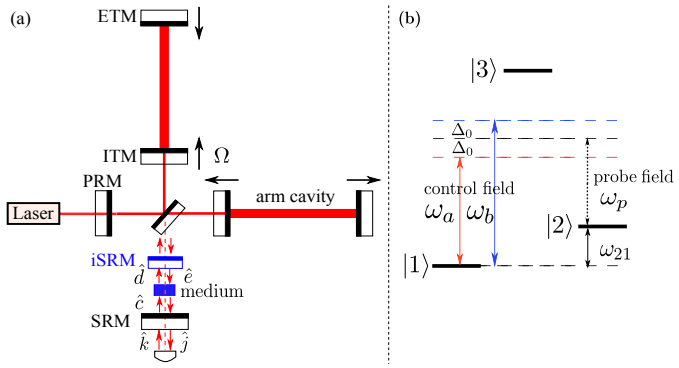

FIG. 1: (Color online)(a) the typical dual recycled interferometer configuration for an advanced gravitational wave detector, with an atomic gain medium (blue block) embedded inside the signal recycling cavity to compensate for the phase delay of the arm cavity. The $\hat{c},\hat{d},\hat{e},\hat{j},\hat{k}$ represent the various light fields in and around the signal recycling cavity. An internal SRM (iSRM) with the same transmissivity as the ITM is introduced to ensure impedance matching so that we can effectively view the compound mirror (consisting of ITM and iSRM) as transparent to the sideband field [13]; (b) the energy levels of the gain medium atoms. Two far-detuned strong control laser beams with frequencies ω_a and ω_b couple the energy levels $|3\rangle$ and $|1\rangle$. The probe field which carries the gravitational wave signal interacts with $|2\rangle$ and $|3\rangle$.

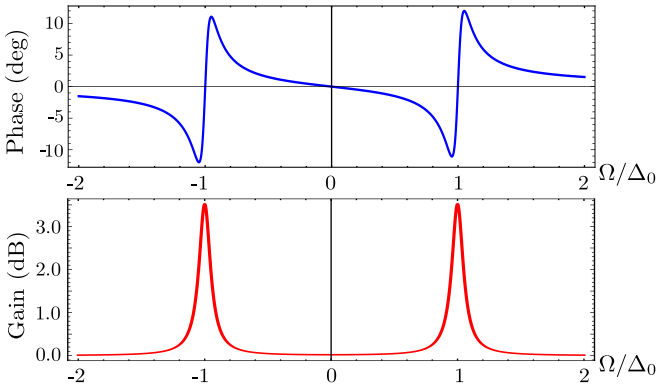

FIG. 2: (Color online) An example of phase angle and amplitude gain of the sideband field propagating through the atomic gain medium, as functions of the normalized (by Δ_0) sideband frequency. The top figure shows the negative dispersion of the atomic gain medium. The white light cavity bandwidth is the linear region between $-\Delta_0$ and Δ_0. The bottom figure shows that the gain is negligibly small, except when $\Omega \sim \pm\Delta_0$. In these frequency regions, the gain is high and this needs to be considered in the design to prevent the possible instability (See Section III for detailed analysis).

Besides the effect of the additional noise, placing a gain medium inside a resonant cavity could cause lasing instability. The effect of this instability to the gravitational wave detector designs has not been discussed in the previous literatures. As we shall see in this paper, the stability requirements put a very strong constraint on the choice of the system parameters.

In this paper, based on a double-pumped three-level atomic medium as shown in Fig. 1, we investigate how the quantum noise and associated gain influence the detector sensitivity and dynamics in a consistent manner. We develop an input-output formalism for the optical field propagating through the gain medium by analyzing the system's Heisenberg equation of motion. Using this formalism, we make a detailed analysis of the quantum shot–noise–limited sensitivity for a typical gravitational wave detector configuration implementing the white light cavity idea, as shown in Fig. 1. Specifically, we consider: (i) the requirement for canceling the propagation phase shift; (ii) the optical stability of the interferometer system with the gain medium; (iii) the noise associated with the amplification process. Taking these factors into account, we find that the integrated shot–noise–limited sensitivity is still limited by Eq. (1) when the gain medium itself is stable (not lasing).

II. A BRIEF SUMMARY

Before presenting the detailed analysis, we briefly summarize our main results in this Section. The susceptibility of the double-pumped gain medium $\chi(\Omega)$ that we derive is given by (the same as in Refs. [14, 16] but with slightly different notation):

$$\chi(\Omega) = \frac{4i\Gamma_{\rm opt}}{i(\Omega+\Delta_0)-\gamma_{12}+\Gamma_{\rm opt}} + \frac{4i\Gamma_{\rm opt}}{i(\Omega-\Delta_0)-\gamma_{12}+\Gamma_{\rm opt}}, \tag{2}$$

where Δ_0 is one half of the frequency difference between the two control fields, and Ω is the sideband frequency of the probe field with carrier frequency ω_p. The damping rate γ_{12} is the effective atomic transition rate from state $|2\rangle$ to $|1\rangle$, while $\Gamma_{\rm opt}$, which depends on the pumping power of the control fields, is the transition rate between $|1\rangle$ to $|2\rangle$ mediated by a virtual excitation of $|3\rangle$. In terms of χ, the ingoing and outgoing fields $\hat{a}_{\rm in}$, $\hat{a}_{\rm out}$ are related by (temporarily ignoring an additional noise term that will be mentioned later):

$$\hat{a}_{\rm out}(\Omega) = [1+i\chi(\Omega)/2]\hat{a}_{\rm in}(\Omega). \tag{3}$$

Under the weak-coupling approximation: $|\chi(\Omega)/2| \ll 1$, the input-output relation Eq. (3) for an unidirectional sideband field passing through the gain medium can be approximated by $\hat{a}_{\rm out}(\Omega) \approx e^{i\chi_r(\Omega)/2}e^{-\chi_i(\Omega)/2}\hat{a}_{\rm in}(\Omega)$. Here, $\chi_r(\Omega)$ and $\chi_i(\Omega)$ are the real and imaginary parts of the susceptibility $\chi(\Omega)$ of the medium, which describe, respectively, the phase accumulation and the amplitude change of the sideband field after passing through the medium. An example is shown in Fig. 2.

In order to compensate for the round-trip propagation phase delay inside the arm cavity, which broadens the bandwidth of the optical cavity, the susceptibility should satisfy $d\chi_r(0)/d\Omega \approx -2L_{\rm arm}/c$ (negative dispersion), which leads to:

$$\frac{2\Gamma_{\rm opt}[(\gamma_{12}-\Gamma_{\rm opt})^2-\Delta_0^2]}{[(\gamma_{12}-\Gamma_{\rm opt})^2+\Delta_0^2]^2} = -\frac{L_{\rm arm}}{c}. \tag{4}$$

Once we fix the parameters $\Gamma_{\rm opt}$ and γ_{12}, we will have a pair of roots for Δ_0^2. For the positiveness of these Δ_0^2, the following

condition has to be satisfied (see Appendix B for a detailed derivation):

$$(\gamma_{12}-\Gamma_{\rm opt})^2 < \Gamma_{\rm opt} c/(4L_{\rm arm}). \tag{5}$$

Under these two conditions in Eq. (4) and (5), we explore the relevant parameter regime for studying the dynamical behavior of the gain medium. Firstly, as we analyze in detail in Sections III and IV(A), the system has two different types of instability (i.e lasing): 1) if $\gamma_{12} < 2\Gamma_{\rm opt}$, there will be a population inversion between levels $|1\rangle$ and $|2\rangle$, and the gain medium starts lasing by itself, which we name "**atomic instability**"; 2) if the photon loss rate for each round trip inside the cavity is less than the photon increasing rate through the amplification by the gain medium, the cavity-medium system starts lasing, which we name "**optical instability**". In Fig. 3, we plot the phase diagram for the stability of the system. This Figure gives a constraint on the possible parameter region for γ_{12} and $\Gamma_{\rm opt}$ of the atomic gain medium (with fixed SRM reflectivity r_s), if lasing were to be avoided. Note that we choose the re-scaled parameters $(\eta = 2\Gamma_{\rm opt}/\gamma_{12}, \xi = 4(\gamma_{12}-\Gamma_{\rm opt})^2 L_{\rm arm}/c\Gamma_{\rm opt})$ instead of $(\gamma_{12}, \Gamma_{\rm opt})$ and survey them within the range $0 < \eta, \xi < 1$. These new parameters help us exclude the atomic instability region ($\eta > 1$) and the region where the phase-cancelation condition is failed ($\xi > 1$).

Secondly, as implied by the above input-output relation, the gain medium is a parametric amplifier. Therefore, as first discussed by Caves [21], there must be an additional noise term in the input-output relation of the probe field to ensure that the commutation relation for $\hat{a}_{\rm out}$ is still $[\hat{a}_{\rm out}(t), \hat{a}^\dagger_{\rm out}(t')] = \delta(t-t')$. As we will show, this additional noise is due to quantum fluctuations that cause spontaneous transitions between $|1\rangle$ and $|2\rangle$, thus degrading the signal–to–noise ratio. From the Hamiltonian, we can derive the noise terms from the Heisenberg equations of motion. Their effect on the integrated shot–noise–limited sensitivity improvement factor (defined in Eq. (36)) is given in Fig. 4 (with tunable parameters of the gain medium, and fixed SRM reflectivity).

From these two Figures, it is clear that: 1) the stability condition and the phase cancelation condition put a strong constraint on the possible parameter region; 2) there is no parameter region where the shot-noise limited sensitivity is improved. This indicates that placing a stable double-pumped gain medium with anomalous dispersion inside the signal recycling cavity cannot broaden the detection bandwidth while also increasing the shot–noise–limited sensitivity. Therefore, one should explore other types of gain media or different parameter regimes to realize the white light cavity idea.

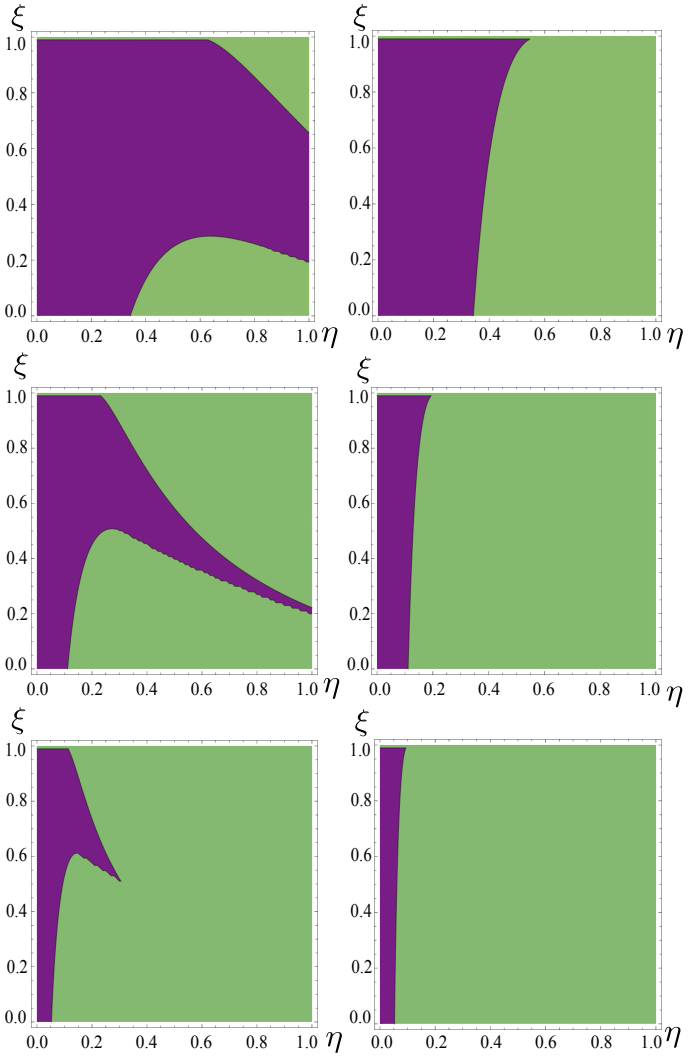

FIG. 3: (Color online) Stability region of the full interferometer scheme with double-pumped gain medium (optical stability only). The SRM power reflectivity $r_s^2 = 0.5, 0.8, 0.9$ are chosen from the top to the bottom panels, while we survey the parameter region for $\Gamma_{\rm opt}, \gamma_{12}$. The horizontal and vertical axes are $\eta = 2\Gamma_{\rm opt}/\gamma_{12}$ and $\xi = 4(\gamma_{12}-\Gamma_{\rm opt})^2 L_{\rm arm}/c\Gamma_{\rm opt}$. We survey η, ξ between 0 and 1 so that atomic instability is excluded and the phase cancellation condition can be satisfied. For each r_s, the left and right panels correspond to the two roots of Δ_0^2 in Eq. (4), respectively. The purple region is the only stable region. In the green region ("optical instability region"), the gain medium is stable by itself but the dynamics of the full interferometer system is unstable (see Section IV for details). With increasing of the SRM reflectivity, the stable region shrinks due to the enhancement of the optical instability effect.

III. INPUT-OUTPUT RELATION OF DOUBLE GAIN ATOMIC MEDIUM

After summarizing the main results, we now start a detailed discussion by first developing an input-output formalism for light propagating through the double-pumped gain medium in the Heisenberg picture. The obtained input-output relation is later combined with that of the main interferometer for evaluating the sensitivity (see Section IV).

As we have briefly mentioned in the Introduction, our gain medium consists of three-level atoms schematically shown in Fig. 1, with two red (blue)-detuned (with respect to the frequency difference between $|3\rangle$ and $|1\rangle$) control lasers. The polarizations of the control and probe fields are orthogonal to each other, and are only sensitive to the atomic transitions between $|1\rangle \leftrightarrow |3\rangle$ and $|2\rangle \leftrightarrow |3\rangle$, respectively. In modeling the gain medium, we treat the atoms as non-interacting distin-

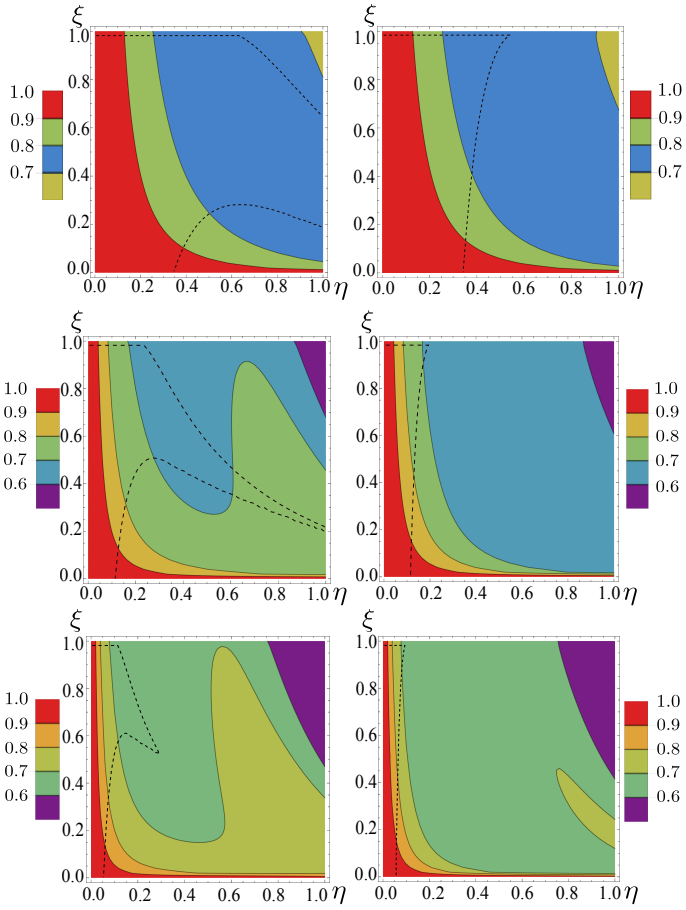

FIG. 4: (Color online) Integrated shot–noise–limited sensitivity improvement factor (defined in Eq. (36)) of the full interferometer scheme with double-pumped gain medium, taking into account the effect of additional noise. The specifications for the parameters is identical to those for Fig. 3. The left and right panels correspond to the two roots of Eq. (4). The dashed line is the boundary of the stable region shown in Fig. 3. It is clear from this Figure that there is no parameter region where the integrated shot–noise–limited sensitivity improvement factor is larger than 1, when the double-pumped gain medium itself is stable.

guishable particles. Nevertheless, all the atoms have the same energy level structures. In this Section, we first derive the atomic dynamics for a single three-level atom, and then extend this result to the many-atoms case under the approximation that the length of the gain medium is much smaller than the spatial scale $2\pi c/\Omega$ of the optical sideband field, where Ω is the gravitational wave frequency.

A. Single-atom dynamics

The above physical modeling leads to the following system Hamiltonian for a single atom:

$$\hat{H} = \hat{H}_{\rm atom} + \hat{H}_f + \hat{H}_{\rm int} + \hat{H}_\gamma. \tag{6}$$

The $\hat{H}_{\rm atom}$ is the free Hamiltonian for a three-level atom in the form of:

$$\hat{H}_{\rm atom} = \sum_{a=1,2,3} \hbar\omega_a \hat{\sigma}_{aa}, \tag{7}$$

where ω_a is the Bohr frequency of energy level a and $\hat{\sigma}_{aa}$ is the atomic population operator.

The $\hat{H}_f$ is the free Hamiltonian for the sideband probe fields propagating in the main gravitational wave detector. Since we are only interested in the optical modes that are around the central frequency of the probe field ω_p, these modes have frequency $\omega_p \pm \Omega$ where Ω denotes the frequency sideband that we are focusing on. Then we have the Hamiltonian $\hat{H}_f$ as:

$$\begin{aligned} \hat{H}_f &= \hbar c \int_{-k_p}^{\infty} dk'(k_p+k')\hat{a}^\dagger_{-k_p-k'}\hat{a}_{-k_p-k'} \\ &\approx \hbar c \int_{-\infty}^{\infty} dk'(k_p+k')\hat{a}^\dagger_{-k_p-k'}\hat{a}_{-k_p-k'}, \end{aligned} \tag{8}$$

where we have assumed that the probe field propagates uni-directionally (along the negative $x-$direction) and $k_p = \omega_p/c, k' = \Omega/c$. We have also used the narrow band approximation $k'/k_p = \Omega/\omega_p \ll 1$ so that we can extend the integral range to $[-\infty,\infty]$. By Fourier transforming the optical creation/annihilation operators to the coordinate domain as: $\hat{a}_x = \int_{-\infty}^{\infty} dk' \hat{a}_{-k_p-k'} e^{-ik'x}$, the above Hamiltonian can be written as (for details, see [24, 25] or Appendix A):

$$\hat{H}_f = \frac{i\hbar c}{2}\int_{-\infty}^{\infty}\left[\frac{\partial \hat{a}_x^\dagger}{\partial x}\hat{a}_x - \hat{a}_x^\dagger\frac{\partial \hat{a}_x}{\partial x}\right]dx. \tag{9}$$

Note that the $\hat{a}_x$ is a slowly varying amplitude operator (both spatially and temporally) with respect to $e^{-i\omega_p x/c - i\omega_p t}$, and it is related to the electric field operator $\hat{E}_p(t)$ as: $\hat{E}_p(t,x) = \hat{a}_x(t)e^{-i\omega_p x/c - i\omega_p t} + h.c.$ The probe field encounters and interacts with the atom at position x_0. This interaction is given by a Jaynes-Cumming type of Hamiltonian under the rotating wave approximation [22]:

$$\hat{H}_{\rm int} = -\frac{\hbar}{2}\mu_{23}\hat{a}^\dagger_{x_0}e^{i\omega_p t}\hat{\sigma}_{23} - \frac{\hbar}{2}\mu_{13}E_c^*\hat{\sigma}_{13} + h.c., \tag{10}$$

where the first term describes the atomic transition between $|2\rangle$ and $|3\rangle$ under the driving of probe fields with transition operator $\hat{\sigma}_{23}$ and the second term describes the atomic transition between $|1\rangle$ and $|3\rangle$ under the pumping of control fields with the transition operator $\hat{\sigma}_{13}$. Here $E_c = E_a e^{i\omega_a t} + E_b e^{i\omega_b t}$ is the sum of the two classical amplitudes of control fields with frequencies $\omega_{a,b}$, and the $\mu_{mn}(m,n=1,2,3)$ are the dipole moments of the atom. We introduce the ladder operator $\hat{\sigma}_{mn}$ describing the atomic state transition from energy level $|n\rangle$ to $|m\rangle$, which satisfies the following algebra:

$$\hat{\sigma}_{mn}\hat{\sigma}_{kl} = \hat{\sigma}_{ml}\delta_{nk}\ ;\ (\hat{\sigma}_{mn})^\dagger = \hat{\sigma}_{nm}. \tag{11}$$

The coupling between an atom with other bath sources at position x_0 is introduced phenomenologically by:

$$\hat{H}_\gamma = i\hbar\sqrt{2\gamma_{12}}\hat{n}^\dagger_{12}e^{i\omega_{21}t}\hat{\sigma}_{12} - \frac{\hbar}{2}\mu_{13}\hat{a}^\dagger_c e^{i\omega_0 t}\hat{\sigma}_{13} + h.c. \tag{12}$$

Here ω_0 is defined as $\omega_0 = (\omega_a + \omega_b)/2$. The $\hat{a}_c$ is the quantum fluctuation associated with the control field. In our 1-D model, the quantum fluctuation associated with the probe field has been included in the $\hat{a}_{x_0}$ field of Eq. (10). The $\hat{n}_{12}$ is the noise bath operator which couples to the atomic transition operator between $|1\rangle$ and $|2\rangle$. This noise bath can be attributed to mutual collisions of atoms or to the stimulation of the external electromagnetic vacuum bath. Here, to study the minimal additional noise, we consider an effectively zero-temperature external bath.

With the full system Hamiltonian, we can now analyze the dynamics of the gain medium. The Heisenberg equation of motion for the probe field derived from Eq. (9) can be written as:

$$\frac{\partial \hat{a}_x}{\partial t} - c\frac{\partial \hat{a}_x}{\partial x} = \frac{i}{2}\mu_{23}\hat{\sigma}_{23}e^{-i\omega_p t}\delta(x-x_0), \tag{13}$$

which reflects the fact that the probe field propagates from right to left (unidirectional) and interacts with atoms at x_0.

We can integrate the above equation around x_0 and obtain:

$$-\hat{a}_{x_0+} + \hat{a}_{x_0-} = \frac{i}{2}\mu_{23}\hat{\sigma}_{23}, \tag{14}$$

in which the $\hat{a}_{x_0+}$ and $\hat{a}_{x_0-}$ are the incoming and outgoing sideband fields (respectively) defined in the vicinity of the interaction point x_0 (in the following, we will use $\hat{a}_{\rm in}$ and $\hat{a}_{\rm out}$ to represent them, respectively). The probe field at x_0 in Eq. (10) and the following Eq. (16) is connected with these vicinity fields through the junction condition:

$$\hat{a}_{x_0} = \frac{1}{2}(\hat{a}_{\rm in} + \hat{a}_{\rm out}). \tag{15}$$

The Heisenberg equations of motion for the atomic transition operators of a single atom in this gain medium are given by:

$$\begin{aligned}
&\dot{\hat{\sigma}}_{13} + (i\omega_{31} + \gamma_{13})\hat{\sigma}_{13} = i\sqrt{2\gamma_{13}}(\hat{\sigma}_{11} - \hat{\sigma}_{33})\hat{a}_{c\rm in}e^{-i\omega_0 t} \\
&\qquad + \frac{i}{2}\mu_{13}(\hat{\sigma}_{11} - \hat{\sigma}_{33})E_c + \frac{i}{2}\mu_{23}\hat{\sigma}_{12}\hat{a}_{x_0}e^{-i\omega_p t}, \quad (16a)\\
&\dot{\hat{\sigma}}_{23} + (i\omega_{32} + \gamma_{23})\hat{\sigma}_{23} = \frac{i}{2}\mu_{13}\hat{\sigma}_{21}(E_c + \hat{a}_c e^{-i\omega_0 t}) \\
&\qquad + i\sqrt{2\gamma_{23}}(\hat{\sigma}_{22} - \hat{\sigma}_{33})\hat{a}_{\rm in}e^{-i\omega_p t}, \quad (16b)\\
&\dot{\hat{\sigma}}_{12} + (i\omega_{21} + \gamma_{12})\hat{\sigma}_{12} = -\sqrt{2\gamma_{12}}(\hat{\sigma}_{11} - \hat{\sigma}_{22})\hat{n}_{12\rm in}e^{-i\omega_{21} t} \\
&\qquad + \frac{i}{2}\mu_{23}\hat{\sigma}_{13}\hat{a}^\dagger_{x_0}e^{i\omega_p t} - \frac{i}{2}\mu_{13}\hat{\sigma}_{32}(E_c + \hat{a}_c e^{-i\omega_0 t}). \quad (16c)
\end{aligned}$$

Note that the $\hat{n}_{12\rm in}$, $\hat{a}_{\rm in}$ and $\hat{a}_{c\rm in}$ are the incoming noise fields, whose relations with the $\hat{n}_{12}, \hat{a}, \hat{a}_c$ of Eq. (12) are given in the way of Eq. (14) and (15). The $\gamma_{13} = \mu_{13}^2/8, \gamma_{23} = \mu_{23}^2/8$ can be derived from Eq. (12). Also, the condition that the majority of atoms are initially prepared at $|1\rangle$ is set as an assumption. In a real experiment, this population preparation can be achieved through various methods such as introducing an additional optical pumping field [16].

It is clear that the above equations of motion are generally nonlinear. However, the system dynamics can be simplified by exploring the linear regime where the scheme is proposed to operate. The simplification can be done using a perturbative method by noting that: 1) the control fields have large detuning with respect to ω_{31}, and therefore the population of atoms on $|3\rangle$ remains small compared to that on $|1\rangle$; 2) the transition between $|1\rangle - |3\rangle$ is much stronger than the transitions between $|1\rangle - |2\rangle$ and $|2\rangle - |3\rangle$ since it is induced by strong control beams; 3) the probe field is very weak compared to the control field since it is around the quantum level.

There are two dimensionless expansion parameters in this system of equations of motion: $\varepsilon \sim \mu_{mn}E_c/\Delta_0, \alpha \sim \mu_{mn}\hat{a}/\Delta_0$ and $\alpha \ll \varepsilon \ll 1$ (note that the denominator could also be other frequency scales such as $\omega_{31} - \omega_{a,b}$; we choose the smallest one here for briefness). Writing the $\hat{\sigma}_{13}$, $\hat{\sigma}_{23}$, $\hat{\sigma}_{12}$ in the rotating frames of ω_0, ω_p and $\omega_0 - \omega_p$, respectively, the leading order ($\sim \varepsilon$) of $\hat{\sigma}_{13}$ dynamics can be derived as:

$$\dot{\hat{\sigma}}_{13} - i(\omega_0 - \omega_{31} + i\gamma_{13})\hat{\sigma}_{13} = \frac{i}{2}\mu_{13}\bar{\sigma}_{11}(E_a e^{-i\Delta_0 t} + E_b e^{i\Delta_0 t}), \tag{17}$$

in which we can approximate the collective population operator on $|1\rangle$ as $\bar{\sigma}_{11} \approx 1$ and $\bar{\sigma}_{mn}$ is the ensemble average of the quantum expectation value of $\hat{\sigma}_{mn}$. The solution of Eq. (17) is:

$$\bar{\sigma}_{13} \approx \frac{1}{2}\frac{\mu_{13}E_a e^{-i\Delta_0 t}}{\omega_{31} - \omega_a} + \frac{1}{2}\frac{\mu_{13}E_b e^{i\Delta_0 t}}{\omega_{31} - \omega_b}. \tag{18}$$

Here, we have neglected γ_{13} which is assumed to be much smaller than the detuning: $\gamma_{13}/|\omega_{a,b} - \omega_{31}| \ll \varepsilon$. In the same rotating frame, the leading order of the $\hat{\sigma}_{23}$ ($\sim \varepsilon^2\alpha$) and $\hat{\sigma}_{12}$ ($\sim \varepsilon\alpha$) dynamics can be written as:

$$\dot{\hat{\sigma}}_{23} - i(\omega_p - \omega_{32} + i\gamma_{23})\hat{\sigma}_{23} = \frac{i}{2}\mu_{13}\hat{\sigma}_{21}\tilde{E}_c, \tag{19a}$$

$$\dot{\hat{\sigma}}_{12} + \gamma_{12}\hat{\sigma}_{12} = \frac{i}{2}\mu_{23}\hat{a}^\dagger_{x_0}\bar{\sigma}_{13} - \frac{i}{2}\mu_{13}\hat{\sigma}_{32}\tilde{E}_c - \sqrt{2\gamma_{12}}\hat{n}_{12\rm in}, \tag{19b}$$

where $\tilde{E}_c = E_a e^{-i\Delta_0 t} + E_b e^{i\Delta_0 t}$ is the pumping field strength in the rotating frame of ω_0, and we have used the fact that $\omega_0 = \omega_p + \omega_{21}$ (See Fig. 1). We also make use of the fact that $\bar{\sigma}_{11} \approx 1$. In deriving Eq. (19), we also assume that the system parameters satisfy: $\gamma_{23}/|\omega_p - \omega_{32}| \ll \varepsilon^2\alpha$.

The dynamics of $\hat{\sigma}_{32}$ can be **adiabatically eliminated** by solving Eq. (19a):

$$\hat{\sigma}_{32} = \frac{\mu_{13}}{2}\frac{\tilde{E}_c^*}{\omega_{32} - \omega_p}\hat{\sigma}_{12}. \tag{20}$$

In deriving this equation, we assume that $\gamma_{23} \ll \omega_{32} - \omega_p$ and make use of the fact that σ_{12} is a slowly varying amplitude, so that $\dot{\hat{\sigma}}_{32} \approx 0$ in Eq. (19). Substituting the solution Eq. (20) and Eq. (15) into Eq. (19b) and Eq. (14), we can obtain a closed equation set for the system dynamics:

$$\hat{a}^\dagger_{\rm out} = \hat{a}^\dagger_{\rm in} - i(\sqrt{2\gamma_{\rm opta}}e^{i\Delta_0 t} + \sqrt{2\gamma_{\rm optb}}e^{-i\Delta_0 t})\hat{\sigma}_{12}, \tag{21a}$$

$$\begin{aligned}
&\dot{\hat{\sigma}}_{12} + (\gamma_{12} - \gamma_{\rm opta} - \gamma_{\rm optb})\hat{\sigma}_{12} = (\gamma_{2\Delta_0} - i\omega_{\rm opt})\hat{\sigma}_{12} \\
&+ i\left(\sqrt{2\gamma_{\rm optb}}e^{-i\Delta_0 t} + \sqrt{2\gamma_{\rm opta}}e^{i\Delta_0 t}\right)\hat{a}^\dagger_{\rm in} - \sqrt{2\gamma_{12}}\hat{n}_{12\rm in}. \quad (21b)
\end{aligned}$$

This equation set describes the coupling between the composite system (consisting of the atom and the pumping fields) and the probe field. The tiny Stark frequency shift $\omega_{\rm opt} = \mu_{13}^2|E_c(t)|^2/(4(\omega_{32}-\omega_p)) \ll \Delta_0$ on the right hand side of Eq.(21b) can be neglected.

The second term on the right-hand-side of Eq. (21b) is the sum of an anti-damping term $\gamma_{\rm opt}\hat{\sigma}_{12}$:

$$\gamma_{{\rm opt}a(b)} = \frac{\mu_{23}^2\mu_{13}^2}{32}\frac{|E_{a(b)}|^2}{(\omega_{31}-\omega_{a(b)})^2}, \tag{22}$$

and a highly-oscillating term $\gamma_{2\Delta_0}\hat{\sigma}_{12}$:

$$\gamma_{2\Delta_0} = \frac{\mu_{23}^2\mu_{13}^2}{32}\left[\frac{E_aE_b^*e^{2i\Delta_0 t}}{(\omega_{31}-\omega_a)^2}+\frac{E_bE_a^*e^{-2i\Delta_0 t}}{(\omega_{31}-\omega_b)^2}\right]. \tag{23}$$

In the symmetric pumping case when $E_a = E_b = E_0$, and considering the approximation $\Delta_0 \ll \omega_{31}-\omega_{a,b}, \omega_{32}-\omega_p$ (These are good approximations to the situation in the proposed experiments [11, 14, 16]), we have $\gamma_{\rm opta} \approx \gamma_{\rm optb} \approx \gamma_{\rm opt} \approx \mu_{23}^2\mu_{13}^2E_0^2/[32(\omega_{31}-\omega_a)^2]$. When $\gamma_{\rm opta}+\gamma_{\rm optb} \approx 2\gamma_{\rm opt} > \gamma_{12}$, we have the population inversion between energy levels $|1\rangle$ and $|2\rangle$, i.e., the atomic instability mentioned earlier.

Solving the Eqs. (21a) and (21b) in the frequency domain, we can obtain the input-output relation for the probe field:

$$\begin{aligned}\hat{a}_{\rm out}(\Omega) =& \mathscr{M}(\Omega)\hat{a}_{\rm in}(\Omega)+\mathscr{N}_+(\Omega)\hat{n}_{12{\rm in}}^\dagger(\Delta_0-\Omega)\\ &+\mathscr{N}_-(\Omega)\hat{n}_{12{\rm in}}^\dagger(-\Delta_0-\Omega),\end{aligned} \tag{24}$$

with $\mathscr{M}(\Omega)$ and $\mathscr{N}_\pm(\Omega)$ given by:

$$\mathscr{M}(\Omega) = 1-\frac{2\gamma_{\rm opt}}{i(\Omega+\Delta_0)-\gamma_{12}+\gamma_{\rm opt}}-\frac{2\gamma_{\rm opt}}{i(\Omega-\Delta_0)-\gamma_{12}+\gamma_{\rm opt}} \tag{25a}$$

$$\mathscr{N}_\pm(\Omega) = \frac{2\sqrt{\gamma_{12}\gamma_{\rm opt}}}{\pm i\Delta_0 - i\Omega+\gamma_{12}-\gamma_{\rm opt}}. \tag{25b}$$

Note that: 1) $\mathscr{N}_\pm^*(-\Omega) = \mathscr{N}_\mp(\Omega)$; 2) hereafter, for simplicity, we will only consider the symmetric pumping case where $E_a = E_b$, because non-symmetric pumping will only induce an additional rotation in the quadrature plane, which does not affect our main results.

The above input-output relation describes a phase-insensitive parametric amplification process. Therefore, there is an additional noise given by the $\hat{n}_{12{\rm in}}^\dagger$ terms in Eq. (24). This noise comes from the stochastic dynamics of $\hat{\sigma}_{12}$ driven by the noise bath as shown in the last term on the right hand side of Eq. (21b). Note that the additional noise term in Eq.(24) has two frequency channels, which can not be figured out by directly using Caves' theory. The formalism presented here based on solving the dynamics from the full system Hamiltonian allow us to pin down the source of the additional noise, and thus give the correct formula for evaluating the noise contribution.

B. Extension to many-atom case

In the above subsection, we discussed the input-output relation for the probe field interacting with a single atom. In this subsection, we extend the above results to the many-atom case.

Since the size of the gain medium (centimeter scale) is much smaller than the spatial scale of the slowly varying amplitude of the probe field (kilometer scale), the slowly changing amplitude of the probe field interacts with all the atoms together. In this case, the anti-damping rate will be enhanced by a factor of N, where N is the number of atoms [26–28]. The $\mathscr{M}$ coefficients in the above input-output relation can be written as:

$$\mathscr{M}(\Omega) = 1-\frac{2\Gamma_{\rm opt}}{i(\Omega+\Delta_0)-\gamma_{12}+\Gamma_{\rm opt}}-\frac{2\Gamma_{\rm opt}}{i(\Omega-\Delta_0)-\gamma_{12}+\Gamma_{\rm opt}}, \tag{26a}$$

where $\Gamma_{\rm opt} = N\gamma_{\rm opt}$.

The formulation of the additional noise field $\hat{n}_{12{\rm in}}$ in the input-output relation for the many-atoms case has some subtleties, which depend on the specific modeling of the interaction between the noise field and the atoms.

• **Noise interacts with atoms locally—**in this case, each atom is associated with its own noise bath. The noise term $\hat{N}_\pm$ will be represented by:

$$\hat{N}_\pm(\Omega) = \sum_\pm\sum_{j=1}^N \mathscr{N}_\pm(\Omega)\hat{n}_{12{\rm in}}^{j\dagger}(\pm\Delta_0-\Omega), \tag{27}$$

where

$$\mathscr{N}_\pm(\Omega) = \frac{2\sqrt{\gamma_{12}\gamma_{\rm opt}}}{\pm i\Delta_0 - i\Omega+\gamma_{12}-\Gamma_{\rm opt}}. \tag{28}$$

• **Noise interacts with atoms collectively—** in some cases, the noise is introduced through processes where the electromagnetic field amplitude interacts with all the atoms collectively as does the slowly-varying amplitude of the probe field. For example, the γ_{12} is induced by applying an additional pumping laser such as in the experiment done in [11]. In this situation, the noise term $\hat{N}_\pm^{(c)}$ will be represented by:

$$\hat{N}_\pm^{(c)}(\Omega) = \sum_\pm \mathscr{N}_\pm^c(\Omega)\hat{n}_{12{\rm in}}^\dagger(\pm\Delta_0-\Omega), \tag{29}$$

where

$$\mathscr{N}_\pm^c(\Omega) = \frac{2\sqrt{\gamma_{12}\Gamma_{\rm opt}}}{\pm i\Delta_0 - i\Omega+\gamma_{12}-\Gamma_{\rm opt}}. \tag{30}$$

The γ_{12} here (also accordingly in $\mathscr{M}(\Omega)$) should be understood as N times the transition rate from $|2\rangle$ to $|1\rangle$ for one single atom, which is proportional to the intensity of the additional pumping laser in the experiment in [11].

Note that: 1) the input-output relations based on both of these noise models approximately satisfies the bosonic commutation relation $[\hat{a}_{\rm out}(\Omega),\hat{a}_{\rm out}(\Omega')] = \delta(\Omega-\Omega')$ under the weak coupling approximation. For the single-pumping case where $\Delta_0 = 0$, the bosonic commutation relation will be exactly satisfied; 2) more importantly, as we shall see later, the subtleties of the noise model *do not* affect the sensitivity of the gravitational wave detector.

C. Some physical discussion

After deriving the system dynamics and input-output relation, we here give some intuitive discussion of the system dynamics and the additional noise.

Firstly, the "anti-damping" dynamics of $\hat{\sigma}_{12}$ can be understood in the following way: a small number of atoms initially populated on $|1\rangle$ can be pumped to $|3\rangle$ by the detuned control fields, and then jump to $|2\rangle$ due to their interactions with the probe field. During this indirect transition between $|1\rangle$ and $|2\rangle$ mediated by $|3\rangle$, the population of atoms on $|2\rangle$ will increase indefinitely if the decay rate from $|2\rangle$ to $|1\rangle$ is not sufficiently large–a "**population inversion process**". Physically, this process could cause **lasing** ("atomic instability" in Section II) and our approximation will fail as the population on $|2\rangle$ becomes larger than the population on $|1\rangle$. One may argue that this instability will not happen in real experiments with the atom population being prepared using additional pumping fields. However, the thermal collision relaxation rate can be tuned to be small if we decrease the gas temperature, increase the pumping beam waist and fill in the "buffer" gas [14, 23]. In this case, a small transition rate contributed by the optical pumping beam could be sufficient for the population preparation. Therefore, in principle, the lasing could still happen, as long as the control fields are strong enough and $2\Gamma_{\rm opt} > \gamma_{12}$.

Secondly, for the additional noise, the stochastic dynamics driven by $\hat{n}_{12\rm in}$ can be attributable to: 1) the collision of atoms due to Van-der-Waals mutual interactions or thermal collisions [14]; 2) the transition between $|2\rangle - |1\rangle$ induced by environmental black-body radiation; 3) the contribution of the quantum noise associated with the additional optical pumping process as in [11]. In Eq. (24) and Eqs. (26)-(29), the $\hat{a}_{\rm out}$ field contains terms related to the additional noise $\hat{n}_{12\rm in}$ in such a way that the stochastic fluctuations of the populations on $|1\rangle$ and $|2\rangle$ will cause fluctuations of the transitions between $|2\rangle$ and $|3\rangle$, since $\hat{\sigma}_{23}$ is slaved by $\hat{\sigma}_{12}$.

In this Section, we have derived the input-output relation for the sideband probe field propagating through the double gain medium from the full Hamiltonian. We also discussed the opto-atomic dynamics and the origin of the additional noise. In the next Section, we will apply these results to the interferometer configuration shown in Fig. 1 and analyze its strain sensitivity.

IV. INTERFEROMETER WITH GAIN MEDIUM

The propagation of sideband fields inside the interferometer shown in Fig. 1 can be schematically described by the flow chart shown in Fig. 5. Here, we only study the differential mode of this interferometer, which carries the gravitational wave signal and can be mapped into a signal cavity containing a gain medium. In this scheme, an internal signal recycling mirror (iSRM as marked in Fig. 1) is used to effectively remove the frequency response of the arm cavities so that the sideband fields see an input-output relation in the following form (we ignore the optomechanical back-action term by assuming infinitely heavy test masses) [29];

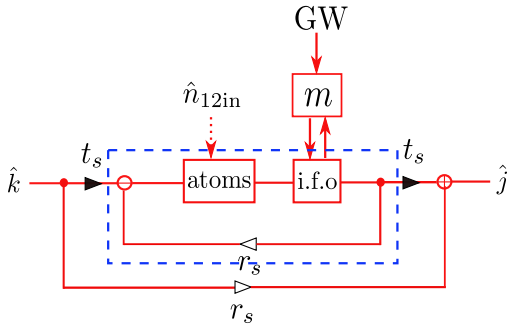

FIG. 5: (Color online) A flow chart showing the propagation of fields in the full system. The i.f.o represents the interferometer modes. The optical stability of the system is determined by the part inside the blue dashed box, whose gain function is given by Eqs. (33) and (34). The test mass (end mirror) m is driven by gravitational waves while the double gain medium is affected by the additional noise $\hat{n}_{12\rm in}$.

$$\hat{e}(\Omega) = e^{2i\Omega\tau}\hat{d}(\Omega) + i\sqrt{\mathscr{K}(\Omega)}e^{i\Omega\tau}h(\Omega), \tag{31}$$

with $\mathscr{K}(\Omega) = P_c\omega_0 L_{\rm arm}^2/(\hbar c^2)$, $\tau = L_{\rm arm}/c$ and $h(\Omega)$ is the strain of the gravitational waves.

The input-output relation for the phase and amplitude quadrature of the light field propagating through the gain medium is (cf. Eq. (26)-(29)):

$$\hat{d}(\Omega) = \mathscr{M}(\Omega)\hat{c}(\Omega) + \hat{N}_+^{(c)}(\Omega) + \hat{N}_-^{(c)}(\Omega), \tag{32}$$

where the forms of the additional noise term $\hat{N}_\pm^{(c)}$ depend on the specific noise modeling, c.f. Eqs. (27)— (30).

The combined effect of the gain medium and the main interferometer can be obtained by substituting Eq. (32) into Eq. (31). Then the final input-output relation for the sideband field is given by:

$$\hat{j}(\Omega) = \hat{j}_n(\Omega) + \hat{j}_s(\Omega), \tag{33a}$$

$$\hat{j}_n(\Omega) = [-r_s + t_s^2 G_c(\Omega)e^{2i\Omega\tau}\mathscr{M}(\Omega)]\hat{k}(\Omega) + t_s e^{2i\Omega\tau}G_c(\Omega)[\hat{N}_+^{(c)}(\Omega) + \hat{N}_-^{(c)}(\Omega)], \tag{33b}$$

$$\hat{j}_s(\Omega) = it_s e^{i\Omega\tau}G_c(\Omega)\sqrt{\mathscr{K}(\Omega)}h(\Omega),, \tag{33c}$$

where $\hat{j}_n$ and $\hat{j}_s$ are the noise and signal parts of the $\hat{j}$ field, respectively. In the above equations, the close-loop gain function

$$G_c(\Omega) = \frac{1}{1 - r_s e^{2i\Omega\tau}\mathscr{M}(\Omega)}, \tag{34}$$

comes from the feedback process due to the reflection of SRM which is shown in the dashed box of Fig. 5, with r_s and t_s being the amplitude reflectivity and transmissivity of the SRM. This feedback process will bring in another potential lasing (the "optical instability" mentioned in Section II) even if $\gamma_{12} > 2\Gamma_{\rm opt}$, as discussed in the following subsection A. The $\hat{k}(\Omega)$ and $\hat{j}(\Omega)$ are the input and output fields of the entire configuration, as shown in Fig. 1 and Fig. 5. The first term

in Eq. (33b) is the quantum noise contributed by the vacuum injection from the outside of the SRM, the second term is the contribution of additional noise introduced by the gain medium.

The output $\hat{j}$ field will be measured by a homodyne detection scheme. In our calculation, we choose the phase quadrature of the output field $\hat{j}_2(\Omega) = [\hat{j}(\Omega) - \hat{j}^\dagger(-\Omega)]/(\sqrt{2}i)$to be measured. Then the shot noise spectrum of the measurement result $S_n^{\rm sh}(\Omega)$ is given by [8]:

$$\pi\delta(\Omega-\Omega')S_n^{\rm sh}(\Omega) = \langle {\rm in}|\hat{j}_{n2}(\Omega)[\hat{j}_{n2}(\Omega')]^\dagger|{\rm in}\rangle_{\rm sym}, \qquad (35)$$

in which the subscript "sym" means replace $\hat{A}(\Omega)\hat{B}^\dagger(\Omega')$ by $\hat{A}(\Omega)\hat{B}^\dagger(\Omega') + \hat{B}^\dagger(\Omega')\hat{A}(\Omega)$, and the $|{\rm in}\rangle$ means the direct product of the vacuum state of the $\hat{k}$ field and the $\hat{n}_{12{\rm in}}$ field. It is technically important to note that both the local noise model and the collective noise model lead to the same sensitivity plots as shown in Fig. 4 and 7 and since we survey all the possible parameter regions of γ_{12} and $\Gamma_{\rm opt}$.

Finally, the shot–noise–limited strain sensitivity $S_{hh}^a(\Omega)$ of the interferometer containing the gain medium is the above noise spectrum Eq. (35) normalized by the signal response. We will discuss the numerical result of this shot-noise limited strain sensitivity in the following subsection B.

A. Stability Criterion

As we have briefly mentioned previously, besides the atomic instability due to the "population-inversion process" when $\gamma_{12} < 2\Gamma_{\rm opt}$, it is important to note that the dynamics of the interferometer with the gain medium may still be unstable (i.e. start lasing) even if $\gamma_{12} > 2\Gamma_{\rm opt}$.

This instability is related to the feedback process discussed below Eq. (33) due to the reflection of the SRM. Intuitively, when the reflectivity r_s of the SRM becomes high (or equivalently, t_s decreases), the photon loss rate through the transmission for each round trip can be less than the photon increasing rate through amplification by the gain medium, corresponding to the **"optical instability"**. The criterion for this instability is determined by the analytical behavior of the closed-loop transfer function Eq. (34). The stability of the full system is determined by the poles of the denominator, which can be obtained by solving the equation $1 - r_s G_o(\Omega) = 0$, where $G_o(\Omega) = e^{2i\Omega\tau}\mathscr{M}(\Omega)$ is the open-loop gain function.

However, the time-elapsed factor $e^{2i\Omega\tau}$ in the gain function makes it difficult to find the root of the above mentioned equation. The **Nyquist criterion** provides us another way to understand the stability through the analytical behavior of $G_o(\Omega)$ [32] (see Appendix C) instead of $G_c(\Omega)$. Specifically, in our system, the Nyquist stability criterion can be stated in such a way that the Nyquist contour of $r_s G_o(\Omega)$ should **not** encircle the point $(1,0)$ in the $({\rm Re}[r_s G_o], {\rm Im}[r_s G_o])$ plane at all. This criterion is equivalent to the lasing condition that the round-trip gain is smaller than one when the phase is an integer multiple of 2π. For illustrative purposes, several examples of the Nyquist contour of $r_s G_o(\Omega)$ are shown in Fig. 6, given typical parameters of γ_{12} and Δ_0. This plot demonstrates that

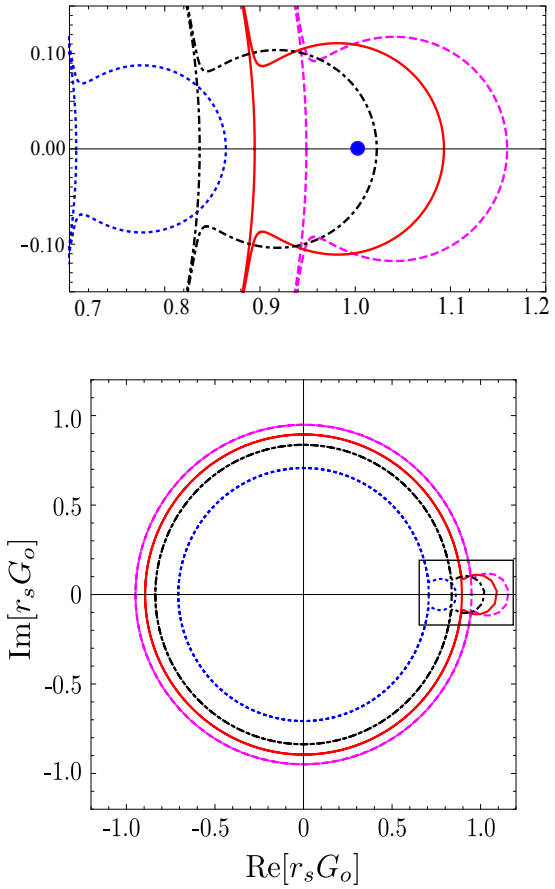

FIG. 6: (Color online) Nyquist contours of $r_s G_o(\Omega)$ for the full system with fixed parameters of the gain medium $\eta = 0.1, \xi = 0.4$, while varying the SRM amplitude reflectivity r_s. The dashed (magenta), solid (red), dotdashed (black), dotted (blue) curves are the Nyquist contours when $r_s^2 = 0.9, 0.8, 0.7$ (unstable cases), and 0.5 (stable cases), respectively. The upper plot shows a magnified view of the contours around (1,0) (the red spot). It is clear here that when the SRM reflectivity increases, the instability develops and the stable region in Fig. 3 shrinks.

increasing the SRM reflectivity can lead to system instability. We further search the parameter region $0 < \eta, \xi < 1$ and give the plot in Fig. 3, from which we can see that the stability criterion imposes a very strong constraint on the possible parameter region.

B. Integrated shot-noise-limited sensitivity improvement factor

To quantitatively describe the improvement of the interferometer sensitivity, we define the integrated shot-noise-limited sensitivity improvement factor (iSNS improvement factor) ρ_r in the following way:

$$\rho_r = \int_0^{\omega_{\rm FSR}} \frac{1}{S_{hh}^a(\Omega)} d\Omega \Big/ \int_0^{\omega_{\rm FSR}} \frac{1}{S_{hh}(\Omega)} d\Omega, \qquad (36)$$

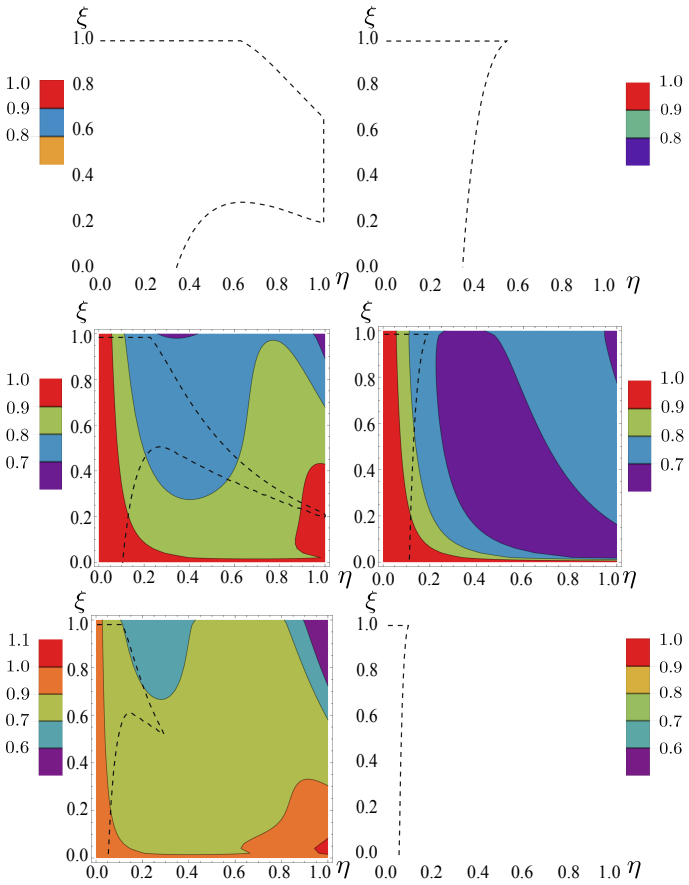

FIG. 7: (Color online) Integrated shot-noise-limited sensitivity improvement factor ρ_r (defined in Eq. (36)) of the full interferometer scheme with double gain medium, without the effect of additional noise. The specifications for the parameters are identical to those for Fig. 3 and Fig. 4. The left and right panels correspond to the larger and smaller roots of Eq. (4), respectively. The dashed line is the boundary of the stable region shown in Fig. 3. In this figure, when the detuning takes the larger solution, there are some regions where $\rho_r > 1$ and the system is stable at the same time. However, as we can see from Fig. 4, these regions will disappear when we take into account the effect of the additional noise.

where S^a_{hh} and S_{hh} (see Eq. (1)) are the shot-noise-limited gravitational wave strain sensitivities of the laser interferometer with a double-pumped gain medium calculated using the method introduced from Eq. (31) to Eq. (35) and that without the gain medium, respectively. In the case $\rho_r > 1$, the system with a double gain medium will improve the signal-to-noise ratio by breaking the trade-off between the detection bandwidth and peak sensitivity. However, we need to be cautious about the stability of the system and the effect of the additional noise at the same time.

We can calculate the strain sensitivity and hence the iSNS improvement factor. By fixing the SRM power reflectivity to be $r_s^2 = 0.5, 0.8, 0.9$, we calculate the iSNS improvement factor by searching the parameter region for (η, ξ) within the range $(0, 1)$, constrained by the phase cancelation condition. For illustrative purposes, we first calculate the ρ_r by ignoring the effect of additional noise introduced by the atom system, and give the resulting plot in Fig. 7. This figure shows that those region where $\rho_r > 1$ is unstable.

However, taking into account the additional noise, the results change in the way that the ρ_r- contours are significantly distorted due to the additional noise, as we can see from Fig. 4. Still, there is no region where the system is stable and $\rho_r > 1$. According to our numerical tests, this conclusion does not change with variation of the SRM reflectivity.

V. CONCLUSION

In this paper, we applied the input-output formalism developed from the Hamiltonian of light-atom interactions to study the quantum noise of a white light cavity using a double gain medium. We find that not only does the additional noise associated with the parametric amplification process affect the system, but that the requirement for the system stability also introduces an additional issue to take into account for its implementation. We conclude that the net sensitivity cannot be enhanced by using the anomalous dispersive behavior of the stable double gain medium when the system is stable. For further study, we will consider the situation that the system is unstable but being controlled by an external feedback loop in an accompanying paper.

Acknowledgments— We thank Atsushi Nishizawa, Bassam Helou, Belinda Pang, and other members of the LIGO-MQM discussion group for fruitful discussions. We thank Vsevolod Ivanov for reading our manuscript and André Fletcher for carefully proofreading the draft thereof. We also thank S. Shahriar for giving useful comments on the manuscript. Y. M. is supported by the Australian Departement of Education, Science and Training. C. Z. is supported by the Australian Research Council. H. M. is supported by the Marie-Curie Fellowship. Y. C is supported by NSF Grants PHY-1068881 and CAREER Grant PHY-0956189. Y. M would like to thank Li Ju and David Blair for their keen support of his visit to Caltech where this work was done.

[1] G. M. Harry, Classical and Quantum Gravity **27**, 84006 (2010).
[2] The Virgo Collaboration, VIR 027A 09 (2009).
[3] K. Somiya, Detector configuration of KAGRA–the Japanese cryogenic gravitational-wave detector, 1111.7185, (2012).
[4] R. X. Adhikari, Rev. Mod. Phys **86**, 121 (2014).
[5] A. Buonanno and Y. Chen, Phys. Rev. D, **65**, 42001 (2002).
[6] A. Buonanno and Y. Chen, Phys. Rev. D, **67**, 62002 (2003).
[7] J. Mizuno., K. A. Strain, P. G. Nelson, J. M. Chen, R. Schilling, A. Rudiger, W. Winkler, and K. Danzmann, Phys. Lett. A **175**, 273 (1993).
[8] H. J. Kimble, Y. Levin, A. B. Matsko, K. S. Thorne, and S. P. Vyatchanin, Phys. Rev. D **65**, 022002 (2001).

[9] A. Wicht, K. Danzmann, M. Fleischhauer, M. Scully, G. Müller, and R.-H. Rinkleff, Optics Communication, **34**, 431, (1997).

[10] A. Wicht, M. Müller, R. H. Rinkleff, A. Rocco, and K. Danzmann, Optics Communications **179**, 107, ISSN 00304018, (2000).

[11] G. S. Pati, M. Salit, K. Salit, and M. S. Shahriar, Phys. Rev. Lett. **99**, 133601, ISSN 0031-9007, 0610022, (2007).

[12] H. N. Yum, J. Scheuer, M. Salit, P. R. Hemmer, and M. S. Shahriar, arXiv:1307.5272, `http://arxiv.org/abs/1307.5272.`, (2013).

[13] M. Salit and M. S. Shahriar, J. Opt. **12**, 104014 (2010).

[14] A. Dogariu, A. Kuzmich, and L. J. Wang, Phys. Rev. A, **63** (5), 053806-12, (2001).

[15] A. M. Akulshin, S. Barreiro, and A. Lezama, Phys. Rev. Lett. **83**, 4277–4280 (1999).

[16] L. J. Wang, A. Kuzmich, and A. Dogariu, Nature **406**, 277-9 (2000).

[17] A. Kuzmich, A. Dogariu, L. J. Wang, P. W. Milonni, and R. Y. Chiao, Phys. Rev. Lett. **86**, 3925 (2001).

[18] Y. Aharonov, B. Reznik, A. Stern, Phys. Rev. Lett., **81**, 2190–2193 (1998).

[19] B. Segev, P. W. Milonni, J. F. Babb and R. Y. Chiao, Phys. Rev. A, **62**, 022114 (2000).

[20] R. W. Boyd, Z. Shi, and P. W. Milonni, J. Opt. **12**, 104007 (2010).

[21] C. M. Caves, Phys. Rev. D **26**, 1817 (1982).

[22] M. O. Scully and M. Suhail-Zubairy, Quantum Optics; Cambridge University Press (1997).

[23] R. Bernheim, Optical Pumping: An Introduction; W.A. Benjamin, New York (1965).

[24] Y. Chen, J. Phys. B: At. Mol. Opt. Phys. **46** 104001 (2013).

[25] T. Hong, H. Yang, H. Miao, and Y. Chen, Phys. Rev. A **88**, 023812 (2013).

[26] D. Polder, Phys. Rev. A **19**, 1192 (1979).

[27] R. H. Dicke, Phys. Rev. **93**, 99 (1954).

[28] E. L. Bolda, R. Y. Chiao, and J. C. Garrison, Phys. Rev. A **52**, 3308 (1995).

[29] A. Buonanno and Y. Chen, Phys. Rev. D **67**, 62002 (2003).

[30] T. Corbitt, Y. Chen, and N. Mavalvala, Phys. Rev. A **72**, 013818 (2005).

[31] C. M. Caves and B. L. Schumaker, Phys. Rev. A **31**, 3068-3092 (1985).

[32] A. B. Pippard, Response and Stability; Cambridge University Press, ISBN 0-521-31994-3 (1985).

Appendix A: Slowly-varying amplitude Hamiltonian of the electromagnetic field

In the main text, the Hamiltonian of the electromagnetic field is given in Eq. (9). Unlike the usual free-field Hamiltonian written in $k-$space, this Hamiltonian is written in $x-$space, and the $\hat{a}_x$ is the slowly varying amplitude of the optical field. In this Appendix, we give a derivation of this form of the Hamiltonian.

In $k-$space, the free-field Hamiltonian for an unidirectional propagating field can be written as:

$$\hat{H}_f = \hbar c \int_{-k_p}^{\infty} dk'(k_p+k')\hat{a}^{\dagger}_{-k_p-k'}\hat{a}_{-k_p-k'}. \tag{A1}$$

Since we are interested in the case $|k'| \ll |k_p|$, we can approximate the above formula as:

$$\hat{H}_f \approx \hbar c \int_{-\infty}^{\infty} dk'(k_p+k')\hat{a}^{\dagger}_{-k_p-k'}\hat{a}_{-k_p-k'}. \tag{A2}$$

This is called the *narrow band approximation*.

Then we can define the optical field operator in $x-$space by Fourier transformation:

$$\hat{a}_x \equiv \int_{-\infty}^{\infty} \hat{a}_{-k_p-k'} e^{-ik'x} dk'. \tag{A3}$$

Substituting the above definition into Eq. (A2), we obtain:

$$\hat{H}_f = \hbar c k_p \int_{-\infty}^{\infty} dx \hat{a}^{\dagger}_x \hat{a}_x + \frac{i\hbar c}{2}\int_{-\infty}^{\infty} dx \left[\frac{\partial \hat{a}^{\dagger}_x}{\partial x}\hat{a}_x - \hat{a}^{\dagger}_x \frac{\partial \hat{a}_x}{\partial x}\right]. \tag{A4}$$

Furthermore, if we work in the rotating frame of ck_0: $\hat{a}_x \to \hat{a}_x e^{-ick_p t}$, then the above Hamiltonian will be:

$$\hat{H}_f = \frac{i\hbar c}{2}\int_{-\infty}^{\infty} dx \left[\frac{\partial \hat{a}^{\dagger}_x}{\partial x}\hat{a}_x - \hat{a}^{\dagger}_x \frac{\partial \hat{a}_x}{\partial x}\right]. \tag{A5}$$

Note that the $\hat{a}_x$ satisfies the commutation relation: $[\hat{a}_x, \hat{a}^{\dagger}_{x'}] = \delta(x-x')$. The $\hat{a}_x$ here is the spatially and temporarily slowly varying amplitude of the electromagnetic field. This fact can be seen from the definition of the electric field under the narrow-band approximation:

$$\begin{aligned}\hat{\tilde{E}}^{(+)}(x,t) &= \hat{E}^{(+)}(x,t)e^{i\omega_0 t + ik_p x} \\ &\approx \sqrt{2\pi\hbar c k_p}\int_{-\infty}^{\infty} dk' \hat{a}_{-k_p-k'} e^{ik'x+ick't} = \sqrt{2\pi\hbar c k_p}\hat{a}_x.\end{aligned} \tag{A6}$$

Appendix B: Phase cancelation condition

For achieving cancelation of the propagating phase inside the arm cavity in the weak coupling limit, the condition below must be satisfied:

$$\frac{2\Gamma_{\rm opt}[(\gamma_{12}-\Gamma_{\rm opt})^2 - \Delta_0^2]}{[(\gamma_{12}-\Gamma_{\rm opt})^2-\Delta_0^2]^2} = -\frac{L_{\rm arm}}{c}. \tag{B1}$$

This condition will reduce to $\Gamma_{\rm opt} = \Delta_0^2 L_{\rm arm}/2c$ when $|\gamma_{12} - \Gamma_{\rm opt}| \ll \Delta_0^2$. In our calculations, we have used the exact formula Eq. (B1).

If we fix the value of γ_{12} and $\Gamma_{\rm opt}$, then the phase cancelation condition becomes a second order algebraic equation for Δ_0^2. Supposing this equation has two roots $(\Delta_0^2)_1$ and $(\Delta_0^2)_2$, then we then have:

$$\begin{aligned}&(\Delta_0^2)_1(\Delta_0^2)_2 = (\gamma_{12}-\Gamma_{\rm opt})^2[(\gamma_{12}-\Gamma_{\rm opt})^2 + 2\Gamma_{\rm opt}c/(L_{\rm arm})], \\ &(\Delta_0^2)_1 + (\Delta_0^2)_2 = 2\Gamma_{\rm opt}c/L_{\rm arm} - 2(\gamma_{12}-\Gamma_{\rm opt})^2.\end{aligned} \tag{B2}$$

Note that in the above equations, $(\Delta_0^2)_1(\Delta_0^2)_2$ is always positive, thereby $(\Delta_0^2)_1 + (\Delta_0^2)_2$ can only be positive:

$$(\gamma_{12}-\Gamma_{\rm opt})^2 < \Gamma_{\rm opt}c/L_{\rm arm}. \tag{B3}$$

On the other hand, Eq. (B1) must have real roots, which gives:

$$(\gamma_{12}-\Gamma_{\rm opt})^2 < \Gamma_{\rm opt}c/(4L_{\rm arm}), \tag{B4}$$

which is a more stringent condition than Eq. (B3).

In summary, considering the requirement of the phase-cancelation condition, our parameters must satisfy Eq. (B4). It is important to note that there are always two Δ_0^2 corresponding to a fixed set of $(\gamma_{12},\Gamma_{\rm opt})$. In plotting the Fig. 4 and Fig. 7, we should take into account both roots.

Appendix C: Nyquist stability criterion

In this Appendix, we give a brief introduction to the Nyquist criterion [32] which we used in understanding the stability condition of the full system in Section IV.

The behavior of control systems is usually described by gain functions. For a control system with a feedback process, the open-loop gain function $G_o(\Omega)$ is used to describe the information transfer ignoring the feedback process, while the closed–loop gain function $G_c(\Omega)$ includes the effect of the feedback process. The relationship between $G_o(\Omega)$ and $G_c(\Omega)$ can be written as:

$$G_c(\Omega) = \frac{G_o(\Omega)}{1+H(\Omega)G_o(\Omega)}. \tag{C1}$$

The $H(\Omega)$ is the gain function for the feedback process itself; it is clear from Fig. 5 that in our system, this is just the reflection of the SRM: $H(\Omega) = -r_s$.

The stability of the system depends critically on the poles of the closed-loop transfer function, i.e, it depends on the poles of $G_o(\Omega)$, and also on the zeros of $1-r_sG_o(\Omega)$. However, computing the poles and zeros of these gain functions is generally a difficult task when they are non-rational. The Nyquist stability criterion is a graphical technique for determining the stability of a control system, which is based on the following *Lemma*: the Cauchy argument principle.

The Cauchy argument principle starts from the Nyquist mapping, which maps the complex argument Ω–plane to the complex $F(\Omega)$–plane. If we have a clockwise contour in the Ω–plane encircling a *zero* of $F(\Omega)$, correspondingly, the contour also encircles the *origin clockwise* in the $F(\Omega)--$plane. However, if we have a clockwise contour in the Ω–plane encircling a *pole*, then the corresponding contour will circulate at the *infinity clockwise* in the $F(\Omega)--$plane, thereby encircling the *origin* in an *anticlockwise* way. In general, if we have a contour in the $F(\Omega)$–plane encircling the origin N times clockwise, that means in the $\Omega--$plane, the number of zeros (Z) and the number of poles (P) satisfy:

$$Z = N + P. \tag{C2}$$

This equality is the Cauchy argument principle.

The Fourier transformation for quantity $A(t)$ between the frequency and time domains is defined as: $A(t) = \int_{-\infty}^{\infty} A(\Omega)e^{-i\Omega t}dt$. Therefore, if $A(\Omega)$ has poles in the upper-half plane, we will have instabilities for a causal system ($t>0$). Now we choose the contour encircling the upper-half $\Omega--$plane as the "Nyquist contour". If the system is stable, then the Z of $1-r_sG_o(\Omega)$ (the denominator of the closed-loop gain function) inside the Nyquist contour should be zero. As a result, the Cauchy argument principle becomes $N=-P$, which is the Nyquist stability criterion.

In our system, with $G_o(\Omega) = \chi(\Omega)e^{2i\Omega\tau}$, we have the the poles of $r_sG_o(\Omega)$ which are $\Omega_{1,2} = \pm\Delta_0 - i(\gamma_{12}-\Gamma_{\rm opt})$. Both of them fall on the outside of the Nyquist contour because $\gamma_{12}-\Gamma_{\rm opt}>0$ for the requirement of the stability of the atomic gain medium itself. Then we can conclude that $P=0$ inside the Nyquist contour. In this case, the Nyquist criterion requires $N=0$ to keep the stability for the full system, i.e, in the Nyquist diagram, the contour of $1-r_sG_o(\Omega)$ should *not* encircle the origin *at all*. In other words, the contour of $r_sG_o(\Omega)$ should not encircle the point $(1,0)$ in the $(\mathrm{Re}[r_sG_o(\Omega)],\mathrm{Im}[r_sG_o(\Omega)])$ plane.